

# Fabrication of quasi-two-dimensional, heterogeneously curved Belousov–Zhabotinsky systems

N. Manz<sup>a)</sup> and S. C. Müller

*Institut für Experimentelle Physik, Abteilung Biophysik, Otto-von-Guericke-Universität, D-39106 Magdeburg, Germany*

(Received 14 April 2003; accepted 9 September 2003)

For many years the Belousov–Zhabotinsky reaction has been used to explore the large variety of dynamical behavior of excitation waves. The understanding of chemical waves can be applied to other physical and biological systems. Most theoretical and experimental work has been done in planar media, whereas for nonplanar systems there exist many theoretical but only very few experimental studies. In this article we present a methodology to develop quasi-two-dimensional, nonhomogeneously curved reaction media. These systems can be used to perform experiments on chemical reaction-diffusion processes which occur, for instance, in the Belousov–Zhabotinsky reaction placed in nonplanar geometries. © 2003 American Institute of Physics.  
[DOI: 10.1063/1.1623623]

## I. REACTION-DIFFUSION SYSTEMS

Excitation waves are common phenomena in many biological, chemical, and physical systems.<sup>1,2</sup> The properties of these waves differ considerably from acoustic or electromagnetic waves in traditional conservative systems. This difference is due to the active local dynamics of excitable media. All these waves, which show spatiotemporal dynamics, can be described by reaction-diffusion (RD) equations including at least one autocatalytic reaction step and the diffusion of the participating components. Wave fronts can appear as circular patterns, as straight or curved lines, or as Archimedean spirals. Important components in all systems are the activator  $u$  and the inhibitor  $v$  having equal or different diffusion coefficients  $D$ . In general the relation  $D_u/D_v \geq 1$  is valid for RD waves. If  $D_v > D_u$ , one can observe time-independent, spatially distributed structures, which are called Turing patterns.<sup>3</sup> This kind of patterns are thought to appear for example on snails and shells<sup>4</sup> or during the growth of plants in water-limited regions.<sup>5</sup>

Let us introduce some examples of excitation waves. In biological systems one can observe waves of cyclic adenosine monophosphate during the chemotactic cell aggregation of the slime mold *Dictyostelium discoideum*,<sup>6</sup> excitation waves on the heart muscle,<sup>7</sup> waves of protons and the coenzyme nicotinamide adenine dinucleotide (NADH) during the glycolysis in yeast cell extracts<sup>8</sup> and neutrophil cells,<sup>9</sup> or  $\text{Ca}^{2+}$  waves at the surface membrane of oocytes of *Xenopus laevis*<sup>10</sup> and after fertilization of human oocytes.<sup>11</sup> Depolarization waves, so called “spreading depression waves,” exist in the neural tissue of the cortex,<sup>12</sup> on the chicken retina,<sup>13</sup> or in the neural tissue of the spinal cord.<sup>14</sup>

The “working horse” for investigations of nonlinear wave propagation is the famous Belousov–Zhabotinsky (BZ)

reaction.<sup>15,16</sup> An example of waves in this reaction is shown in Fig. 1.

This chemical reaction can be used to explore the dynamics of excitation waves, for example, in homogeneous<sup>16</sup> and nonhomogeneous<sup>17</sup> or planar<sup>18</sup> and nonplanar<sup>19,20</sup> systems. The results can be applied to other biological and physical systems by changing the parameters, for example, in coupled three- or two-component differential equation systems, such as the Oregonator model<sup>21</sup> or the Tyson–Fife model,<sup>22</sup> respectively. The first model contains the activator species, the inhibitor species, and the catalyst as variables. In the two-variable system the inhibitor is adiabatically eliminated to obtain a model with the activator and a control variable.

Generally, the BZ reaction can be described as the oxidation of an organic substrate by bromate in an acid solution and in the presence of a redox catalyst. Investigations can be performed in a liquid solution or in a jelled medium. In the latter case the catalyst is immobilized in a gel matrix where the reaction takes place. These systems prevent hydrodynamic convection in the BZ reaction media<sup>23</sup> and make experiments in open Petri dishes possible.<sup>24</sup>

## II. CURVED REACTION-DIFFUSION SYSTEMS

In this article we present a methodology to produce nonplanar quasi-two-dimensional systems. But why is it important to investigate excitation waves in such systems? Up to now most experiments were done in planar RD systems such as in Petri dishes, on membranes, in planar porous glass plates, or in gels between planar permeable membranes to investigate spatio-temporal structures. In these planar geometries the system is assumed to be infinitely extended and characterized by homogeneously or nonhomogeneously distributed parameters.<sup>25</sup>

But in nature, there exist many curved systems. Some of them are introduced in the previous section. In these systems the geometry of the excitable medium has an influence on the dynamics of the spatiotemporal pattern, as first discussed

<sup>a)</sup> Author to whom correspondence should be addressed; present address: Department of Chemistry and Biochemistry, Florida State University, Tallahassee, Florida 32306-4390; electronic mail: nmanz@chem.fsu.edu



FIG. 1. Picture of chemical waves in the Belousov–Zhabotinsky reaction in a Petri dish. A circular pattern and a counter-rotating spiral pair are visible as bright structures in the dark reaction solution.

in 1946 by Wiener and Rosenblueth.<sup>26</sup> Since then, there have been theoretical studies investigating excitation waves in homogeneously<sup>27,28</sup> and nonhomogeneously<sup>29–31</sup> curved systems, exploring a large variety of dynamical behavior.<sup>25</sup>

The investigation of curvature effects starts from at least two aspects. First, there is an influence of the surface curvature on the diffusive coupling of active components. Second, closed surfaces as cylinders and spheres have an influence on the pattern formation. Different periodic boundary conditions have to be considered, which leads to the possibility that wave fronts can reach their origin. Both factors (surface curvature and topology) determine the stability or the existence of specific dynamical conditions that are not possible in infinite extended planar systems.<sup>32</sup>

But there are only a few, not very detailed, experimental results. The first reported observation of excitation waves (spirals) in a curved BZ system was done in 1989.<sup>19</sup> In 1997, Steinbock investigated the propagation of spiral waves on a cylindrical surface.<sup>20</sup> In both experiments the surfaces were homogeneously curved. Only one experimental article reports about the behavior of spirals on a nonhomogeneously curved surface (a paraboloid).<sup>33</sup> The other experiments, which investigated the dynamics of initially planar fronts propagating across a periodically modulated curved surface<sup>34–36</sup> are based on the methodology presented in this article.

### III. FABRICATING CURVED SURFACES

The experimental device containing the quasi-two-dimensional, heterogeneously curved system uses a hollow acrylic glass (e.g., plexiglass) mold with a pair of complementary surfaces. The two curved surfaces, once put together, have a small, constant distance  $\xi$  in normal direction of each point. The procedure of developing and calculating the two surface functions is the main goal of this article. Figure 2 shows one side of such a system with the centered nonhomogeneously curved part.

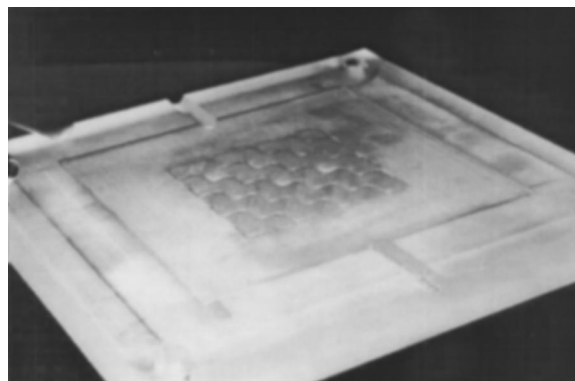


FIG. 2. Picture of one side of an acrylic glass mold. The nonhomogeneously curved region is surrounded by a planar part. Also visible are the channels which are necessary to fill the hollow mold with the BZ solution.

The two surfaces with the central curved part and a surrounding planar region can be visualized with a computer-aided design program and milled with a computer numerical control machine. The thin, hollow space of the mold can accommodate the chemical reaction solution. Because of the different absorption coefficients of the reduced state and the oxidized wave in the BZ reaction, illuminating the transparent system from below enables the detection of wave propagation with a charge-coupled-device camera.

To develop quasi-two-dimensional systems with this methodology one has to choose between two different possibilities. In both cases one has to select an explicit starting function: for a modulated system, for example, the simple, doubly periodical function

$$f(x,y) = A \sin(bx) \sin(by), \quad (1)$$

with amplitude  $A$ , wave number  $b = 2\pi/\lambda$ , and modulation wavelength  $\lambda$ . The Cartesian coordinates are given by  $x$ ,  $y$ , and  $z$ . With such functions one can describe an extended, periodically modulated system<sup>34,35</sup> or single, localized nonhomogeneously curved parts by milling, for example, only one half of the modulation wavelength in  $x$  and  $y$  direction.<sup>37</sup>

The two possible realizations differ in the position of the given starting function  $f$ . The first option is to choose the function for one surface of the system itself. In this case the second, calculated surface has the distance of the thickness  $\xi$  of the system. For the second option, the function is placed precisely between the two surfaces of the hollow mold. In this case one has to calculate both surface functions, each with a distance  $\zeta = \xi/2$  in opposite direction from the starting function, as shown in Fig. 3.

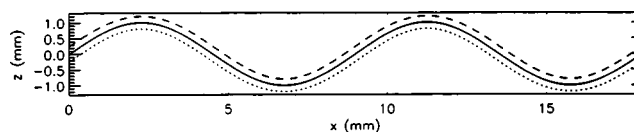


FIG. 3. Two-dimensional scheme of the median surface  $f(x,y) = A \sin(bx) \sin(by)$  (solid line) with  $A = 1.0$  mm and  $b = 2\pi/\lambda = 2\pi/9.0$  mm<sup>-1</sup> and the calculated upper surface  $s_u$  (dashed line) and lower surface  $s_l$  (dotted line) in the  $xz$  plane at  $y = \lambda/4$  of  $f(x,y)$  with a total distance of  $\xi = 0.4$  mm. Axes are not to scale.

Since the calculations for the first case are included in those for the second case, we will confine ourselves to the latter one. The advantages of the second case are explained in Sec. III C with the example of Eq. (1) after the basic calculations have been introduced.

**A. Calculating the surface functions**

Starting with an explicit function  $f(x,y)$ , the upper  $s_u(x,y)$  and lower  $s_l(x,y)$  surface functions of the hollow mold, with a constant distance in normal direction of every point of the starting function, can be expressed only in parametric description.<sup>38</sup>

The surface with the starting function  $f$  is defined by  $\mathbf{k} = [x, y, f(x, y)]^T$ . With the derivatives  $f_x = \partial f(x, y) / \partial x$  and  $f_y = \partial f(x, y) / \partial y$  the opposite normal vectors can be written as  $\mathbf{N}_u = (-f_x, -f_y, 1)^T$  and  $\mathbf{N}_l = (f_x, f_y, -1)^T$ . Using the normalization  $N_n = |\mathbf{N}_u| = |\mathbf{N}_l|$ , one obtains the normalized antiparallel vectors in normal direction  $\mathbf{n}_u = \mathbf{N}_u / N_n$  and  $\mathbf{n}_l = \mathbf{N}_l / N_n$  of  $\mathbf{k}$ . Now one can define the two surface functions by

$$\mathbf{s}_u = \mathbf{k} + \zeta \cdot \mathbf{n}_u \quad \text{and} \quad \mathbf{s}_l = \mathbf{k} + \zeta \cdot \mathbf{n}_l.$$

Remember that the distance  $\zeta$  of each surface from the median surface is half of the total thickness  $\xi$  of the system. The resulting surface functions can be obtained from

$$\mathbf{s}_u = \begin{pmatrix} x - \frac{\zeta \cdot f_x}{\sqrt{f_x^2 + f_y^2 + 1}} \\ y - \frac{\zeta \cdot f_y}{\sqrt{f_x^2 + f_y^2 + 1}} \\ f(x, y) + \frac{\zeta}{\sqrt{f_x^2 + f_y^2 + 1}} \end{pmatrix} \quad \text{and} \quad (2)$$

$$\mathbf{s}_l = \begin{pmatrix} x + \frac{\zeta \cdot f_x}{\sqrt{f_x^2 + f_y^2 + 1}} \\ y + \frac{\zeta \cdot f_y}{\sqrt{f_x^2 + f_y^2 + 1}} \\ f(x, y) - \frac{\zeta}{\sqrt{f_x^2 + f_y^2 + 1}} \end{pmatrix}. \quad (3)$$

**B. The maximal normal distance**

The maximal normal distance  $\zeta$  is not an arbitrary parameter of the system. For every median surface  $\mathbf{k}$  a maximal value  $\zeta_{\max}$  exists. Larger values cause singularities in the calculated surfaces  $\mathbf{s}_u$  and  $\mathbf{s}_l$ . This effect is shown in Fig. 4 in a cross section of the surface of Eq. (1) in the  $xz$  plane at  $y = \lambda/4$ .

To calculate the maximal normal distance from the median surface one has to look for a line through the surface that contains the points where the  $\zeta_{\max}$  values are minimal. For the upper surface these points are the minima of the median surface  $f$ , for the lower surface the maxima. If the

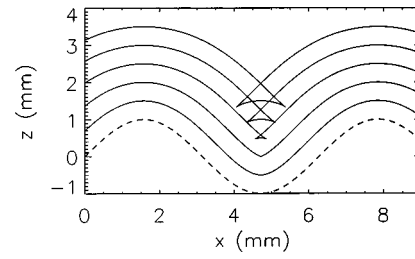


FIG. 4. The median surface  $f(x,y) = A \sin(bx)\sin(by)$  (dashed line) with  $A = 1.0$  mm and  $b = 2\pi/\lambda = 2\pi/9.0$  mm<sup>-1</sup> and the calculated upper surface  $s_u$  in five different normal distances of  $0.5 \leq \zeta \leq 2.5$  (solid lines) in the  $xz$  plane at  $y = \lambda/4$  of  $f(x,y)$ . Axes are not to scale.

minima and maxima have different curvatures, one has to choose the extrema with the highest absolute curvature. In a doubly periodical surface as defined by Eq. (1) one can choose, for example,  $y = \text{const.} = \lambda/4$ . Now one can rewrite Eq. (1) as

$$f(x, y) = A \cdot \sin\left(\frac{2\pi}{\lambda}x\right) \underbrace{\sin\left(\frac{2\pi}{\lambda}y\right)}_{-1 \leq \text{const.} \leq 1} \leq a \cdot \sin\left(\frac{2\pi}{\lambda}x\right) =: \tilde{f}(x). \quad (4)$$

As one can see in Eq. (4) the determination of  $\zeta_{\max}$  can be done with only one variable because of the inequality  $a \geq A$ . In this case Eq. (2) reads with  $f_x = df(x)/dx = \tilde{f}'$  and  $f_y = 0$  as follows:

$$\mathbf{s}_u = \begin{pmatrix} s_1(x) \\ s_2(x) \end{pmatrix} = \begin{pmatrix} x - \frac{\zeta \cdot \tilde{f}'}{\sqrt{\tilde{f}'^2 + 1}} \\ \tilde{f}(x) + \frac{\zeta}{\sqrt{\tilde{f}'^2 + 1}} \end{pmatrix}.$$

To use  $s_2(x)$  as a function of  $s_1(x)$  one has to determine the inverse function  $s_1^{-1}(x)$  and guarantee that this function exists. The following inequality has to hold

$$\frac{(\tilde{f}'^2 + 1)^3}{\tilde{f}''^2} \geq \zeta^2. \quad (5)$$

Because this necessary condition is valid for all  $x$ , one has to find the minima of the left part of Eq. (5) with

$$\frac{d}{dx_0} \left\{ \frac{[\tilde{f}'^2(x_0) + 1]^3}{\tilde{f}''^2(x_0)} \right\} = 0$$

$$\Leftrightarrow 3 \cdot \tilde{f}''^2(x_0) \cdot \tilde{f}'(x_0) - [\tilde{f}'^2(x_0) + 1] \cdot \tilde{f}'''(x_0) = 0. \quad (6)$$

With the condition Eq. (6) one can calculate a  $x_0$  value for the surface function. Inserting this value in Eq. (5), one obtains a maximal distance  $\zeta_{\max}$  which generates useful outer surfaces. Combining both equations yields:

$$\zeta_{\max} = \frac{[\tilde{f}'^2(x_0) + 1]^{3/2}}{\tilde{f}''(x_0)}.$$

### C. Surface curvature

The determination of the curvature in every point of the surfaces is necessary to choose appropriate hemispherical milling heads. The curvature of the milling head always has to be larger than the largest value of the surfaces. Because of the given symmetrical functions it is sufficient to check the surface curvature along a line at, e.g.,  $y = \text{const}$ . For surfaces given in parametric description [ $\tilde{x} = \tilde{x}(x), \tilde{y} = \tilde{y}(x)$ ] one has to use<sup>38</sup>

$$K_{\text{para}}(x) = \frac{\tilde{x}' \cdot \tilde{y}'' - \tilde{x}'' \cdot \tilde{y}'}{(\tilde{x}'^2 + \tilde{y}'^2)^{3/2}}. \quad (7)$$

The primes denote the derivative with respect to  $x$ . For the explicitly given function the curvature can be calculated by

$$K_{\text{expl}}(x) = \frac{\tilde{f}''}{(1 + \tilde{f}'^2)^{3/2}}. \quad (8)$$

Now we will explain why it is better to use as the starting function the median surface with the example Eq. (1). In this case it is also sufficient to check the function along a line which contains the maxima and minima as in Eq. (4).

#### 1. Starting function as a surface

Let us take the lower surface as the given starting function. One has to calculate the corresponding curvature function  $K_1$  for the selected line with Eq. (8). For the upper surface one has to use Eq. (2) with the chosen reduction to a one-dimensional system with

$$\tilde{x}(x) = x - \frac{\zeta \cdot \tilde{f}'}{\sqrt{\tilde{f}'^2 + 1}} \quad (9)$$

and

$$\tilde{y}(x) = \tilde{f} + \frac{\zeta}{\sqrt{\tilde{f}'^2 + 1}}. \quad (10)$$

Inserting Eqs. (9) and (10) into Eq. (7) yields the curvature function  $K_u$  of the upper line. Figure 5 shows the  $z$  values of the two surface functions in  $x$  direction at the chosen  $y$  value and the corresponding curvature functions.

Now two phenomena are conspicuous. First, the curvature of the given function  $f(x, y)$  at  $y = \lambda/4$  is symmetrical with respect to the point at  $f(x) = A \sin(\lambda/2)$  as is the function itself. In this case, the absolute value of the curvature in the minima and maxima are the same according to

$$\left| K_{f(x)} \left( x + \frac{k\lambda}{2} \right) \right| = \text{const.} \quad k \in \mathbb{Z}.$$

Second, the curvature function of the calculated surface differs considerably from the function of the given surface. As a result, the curvature differences (which are unavoidable) in the minima and maxima of the two surfaces are not the same. If the normal distance  $\xi$  is constant, this effect will increase by decreasing the wavelength  $\lambda$  of the given function and vanish if  $\lambda$  is increased.

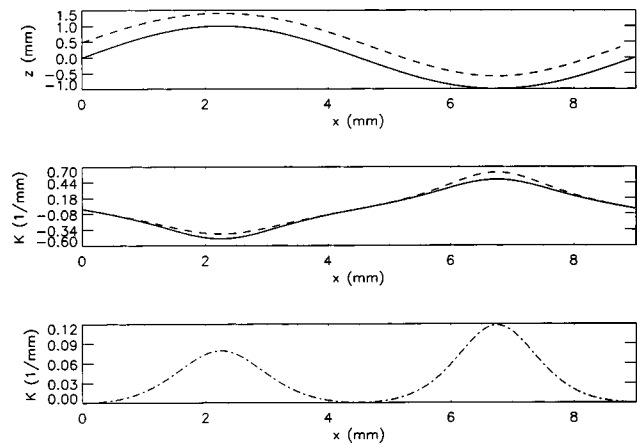


FIG. 5. Upper graph:  $z$  values of the two surface functions in  $x$  direction at  $y = \lambda/4$ . The given function  $f(x, y) = A \cdot \sin(bx) \cdot \sin(by) = s_l$  (solid line) with amplitude  $A$ , wave number  $b = 2\pi/\lambda$ , and the calculated function  $s_u$  (dashed line) are separated by a distance  $\xi$  in normal direction. Parameter values are  $\xi = 0.4$  mm,  $A = 1.0$  mm, and  $\lambda = 9.0$  mm<sup>-1</sup>. Middle graph: Corresponding curvature functions  $K_1$  (solid line) and  $K_u$  (dashed line). Lower graph: Curvature difference  $\Delta K$  between the two functions.

In the minima, the curvature  $K_1$  increases strictly monotonically for  $\lambda \rightarrow \infty$  and is approaching  $\infty$  asymptotically. The behavior of the curvature function  $K_u$  is similar, with the difference that the asymptotic approximation of  $K_u$  at  $\infty$  appears already at a critical wavelength  $\lambda_{\text{crit}}$  defined by Eq. (5) and therein the surface function [e.g., Eq. (4)]. Below this value,  $\lambda_{\text{crit}}$  will obtain singularities in the calculated surface as shown in Fig. 4.

#### 2. Starting function between the surfaces

To reduce the explained curvature differences  $\Delta K$  between the upper and lower surface and, more important, to get the same  $\Delta K$  in the minima and the maxima, one has to define the given function as the median function of the system. In this advantageous case with the same  $\Delta K$  values in all extrema, the upper and lower surface has to be calculated by Eqs. (2) and (3). Such a system is shown in Fig. 3.

Calculating the curvature functions  $K_u$  and  $K_1$  by Eq. (7),  $\Delta K$  results and one obtains the graphs shown in Fig. 6.

A comparison of Figs. 5 and 6 yields two differences:  $\Delta K_{\text{max}}$  is smaller than before and  $\Delta K$  in the maxima and minima have the same values. The latter result is the most important one. Now there is no difference between maxima and minima with respect to the local system curvature for propagating reaction-diffusion waves.

### D. Surface roughness

The surface roughness is an important factor for uncontrolled, potential nucleation points of chemical waves. During the fabrication with cylindrical and hemispherical milling heads, one has to distinguish between two kinds of roughness. One is determined by the milling process itself, namely by the cutting remnant of the milling process. This effect also occurs on planar milling surfaces and can be removed by polishing the surface with an acrylic glass polish paste.

The other roughness with a much larger effect can be minimized by the consideration of some process parameters.

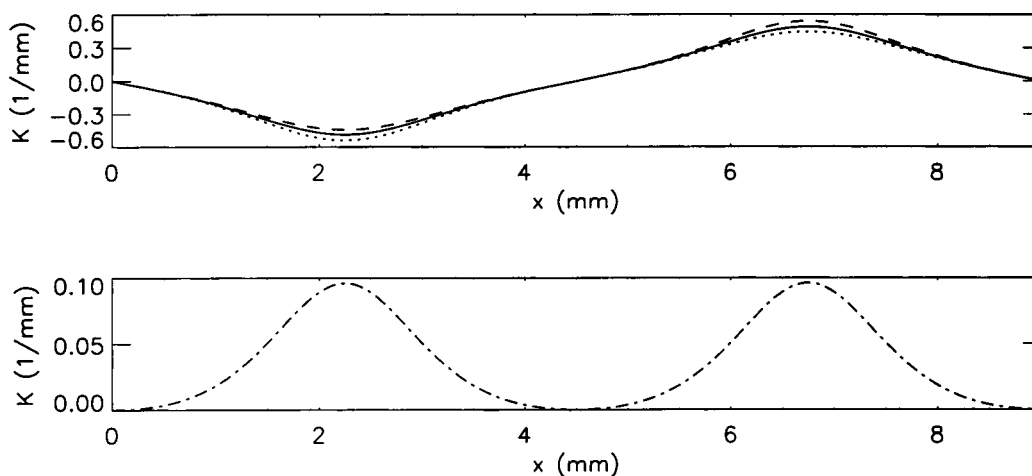


FIG. 6. Upper graph: Curvature functions of the given median function (solid line) and the calculated surfaces  $K_1$  (dotted line) and  $K_u$  (dashed line). Lower graph: Curvature difference  $\Delta K$  between the two outer functions.

This is a result of nonplanar milling heads, which are necessary for the curved surfaces. The maximal unevenness  $\delta$  resulting from hemispherical milling heads can be calculated by

$$\delta = \left( -\sqrt{R^2 - \frac{d^2}{4}} \right) + R, \quad (11)$$

if the curvature  $K$ , respectively, the radius  $R$ , of the chosen milling head and the distance  $d$  between two milling paths are known. With typical values of  $d=0.05$  mm and  $R=0.5$  mm one obtains a surface roughness of  $\delta=0.63$   $\mu\text{m}$ . As a result of Eq. (11) it can be seen that the knowledge of the maximal curvature of the surface makes a reduction of the surface roughness possible. The radius of the milling head has to be chosen as large as possible.

#### IV. USING THE NONPLANAR MOULD

After the fabrication of a quasi-two-dimensional, curved system one can choose several ways to investigate excitation waves in the BZ solution.

##### A. Liquid BZ system

Using a liquid BZ system in a closed mold, one has to adopt the classical BZ system to these conditions. Therefore, one has to ensure that the reaction does not produce  $\text{CO}_2$  as a product. Such “bubble-free” reactions (e.g., Ref. 39) prevent the formation of undesired  $\text{CO}_2$  bubbles in this system. In this case, the liquid BZ solution is poured into the mold. After closing the filling tube and initiating a front, wave propagation can be investigated.

##### B. Closed gel BZ system

In a closed gel system the procedure is the same as for a liquid BZ system. The difference is that the solution contains, for example, a defined amount of waterglass which jells after some time to form a silica gel. In this case one can also use a bubble-free recipe or insert sodium-dodecylsulfate, which reduces the surface tension, to suppress the growing of undesired  $\text{CO}_2$  bubbles. Now the catalyst is immobilized in

the gel matrix and all components are included in the gel. Normally this procedure is used to investigate three-dimensional BZ waves.<sup>40,41</sup>

##### C. Open gel BZ system

Using an open gel system is nearly the same as preparing an experimental setup with Petri dishes. For these experiments the liquid gel with the catalyst has to be poured into the acrylic glass mold. After jelling, the mold must be opened, to reveal the curved gel surface. The gel has to be prepared as usual (e.g., Ref. 42) and can be covered with the liquid BZ solution. To keep a sufficient liquid layer on top of the gel, the use of a frame around the gel is necessary.

##### D. Other systems

In further applications one may think of other chemical systems that produce characteristic propagating fronts for which the stability may strongly depend on the curvature of the surface.

#### V. DISCUSSION

We have presented a procedure to produce quasi-two-dimensional, heterogeneously curved devices for investigating the dynamics of reaction-diffusion waves propagating in nonplanar systems. Up to now, these are mainly applied to nonhomogeneously curved Belousov–Zhabotinsky reaction layers. A remarkable finding has been reported that documents the curvature effect on the excitability of BZ systems. On curved surfaces Davydov *et al.* found a curvature-dependent loss of excitability<sup>35</sup> that causes the breakup of propagating wave fronts. There is certainly a large variety of further examples, for possible use, that have been investigated exclusively in planar geometries.

In further applications one may think of other chemical systems, such as the monostable or bistable arsenous acid reaction, in which characteristic propagation fronts occur. The stability of these fronts may also sensitively depend on the the curvature of the surface they are crossing. In the context of investigating viscous fingering in Hele–Shaw

cells<sup>43</sup> De Wit has considered theoretically the behavior of front propagation in cells of periodically varying thickness.<sup>44</sup> A corresponding experimental study of a chemical front propagating in such a cell geometry is underway. Finally, applications to front propagation in biological systems as in bacterial colonies,<sup>45</sup> for example, are of major interest.

## ACKNOWLEDGMENTS

This work was supported by the Deutsche Forschungsgemeinschaft and the Max-Planck-Institut für Physik komplexer Systeme. The authors thank the Otto-von-Guericke Universität Magdeburg (Institut für Fertigungstechnik und Qualitätssicherung) for technical support and especially Ulrich Storb for many fruitful discussions.

- <sup>1</sup>R. Kapral and K. Showalter, *Chemical Waves and Patterns* (Kluwer Academic, Dordrecht, 1995).
- <sup>2</sup>J. D. Murray, *Mathematical Biology*, 3rd ed. (Springer, Berlin, 2002).
- <sup>3</sup>A. M. Turing, *Philos. Trans. R. Soc. London, Ser. B* **237**, 37 (1952).
- <sup>4</sup>H. Meinhardt and M. Klingler, *J. Theor. Biol.* **187**, 63 (1987).
- <sup>5</sup>J. von Hardenberg, E. Meron, M. Shachak, and Y. Zarmi, *Phys. Rev. Lett.* **87**, 198101 (2001).
- <sup>6</sup>F. Siegert and C. J. Weijer, *J. Cell. Sci.* **93**, 325 (1989).
- <sup>7</sup>R. A. Gray, A. M. Pertsov, and J. Jalife, *Nature (London)* **392**, 75 (1998).
- <sup>8</sup>T. Mair and S. C. Müller, *J. Biol. Chem.* **271**, 627 (1996).
- <sup>9</sup>H. R. Petty and A. L. Kindzelskii, *Proc. Natl. Acad. Sci. U.S.A.* **98**, 3145 (2001).
- <sup>10</sup>J. Lechleiter, S. Girard, E. Peralta, and D. Clapham, *Science* **252**, 123 (1991).
- <sup>11</sup>J. Tesarik, M. Sousa, and J. Testart, *Hum. Reprod.* **9**, 511 (1994).
- <sup>12</sup>A. A. P. Leão, *J. Neurophysiol.* **7**, 359 (1944).
- <sup>13</sup>N. A. Gorelova and J. Bureš, *J. Neurobiol.* **14**, 353 (1983).
- <sup>14</sup>D. S. Streit, C. R. Ferreira, and H. Martins-Ferreira, *J. Neurophysiol.* **74**, 888 (1995).
- <sup>15</sup>A. M. Zhabotinsky, *Biophysics (Engl. Transl.)* **9**, 329 (1964).
- <sup>16</sup>A. N. Zaikin and A. M. Zhabotinsky, *Nature (London)* **225**, 535 (1970).
- <sup>17</sup>V. G. Morozov, N. V. Davydov, and V. A. Davydov, *J. Biol. Phys.* **25**, 87 (1999).
- <sup>18</sup>E. Meron, *Phys. Rep.* **218**, 1 (1992).

- <sup>19</sup>J. Maselko and K. Showalter, *Nature (London)* **339**, 609 (1998).
- <sup>20</sup>O. Steinbock, *Phys. Rev. Lett.* **78**, 745 (1997).
- <sup>21</sup>R. J. Field and R. M. Noyes, *J. Chem. Phys.* **60**, 1877 (1974).
- <sup>22</sup>J. J. Tyson, *Ann. N.Y. Acad. Sci.* **316**, 279 (1979).
- <sup>23</sup>H. Miike, S. C. Müller, and B. Hess, *Phys. Rev. Lett.* **61**, 2109 (1988).
- <sup>24</sup>T. Yamaguchi, L. Kuhnert, Zs. Nagy-Ungvarai, S. C. Müller, and B. Hess, *J. Phys. Chem.* **95**, 5831 (1991).
- <sup>25</sup>V. S. Zykov, *Simulation of Wave Processes in Excitable Media* (Manchester University Press, New York, 1987).
- <sup>26</sup>N. Wiener and A. Rosenblueth, *Arch. Inst. Cardiol. Mex.* **16**, 205 (1946).
- <sup>27</sup>P. K. Brazhnik, V. A. Davydov, and A. S. Mikhailov, *Theor. Math. Phys.* **74**, 300 (1988).
- <sup>28</sup>V. S. Zykov and S. C. Müller, *Physica D* **97**, 322 (1996).
- <sup>29</sup>V. A. Davydov and V. S. Zykov, *Physica D* **49**, 71 (1991).
- <sup>30</sup>J. M. Rogers, *Chaos* **12**, 779 (2002).
- <sup>31</sup>V. A. Davydov, V. G. Morozov, and N. V. Davydov, *Phys. Lett. A* **307**, 265 (2003).
- <sup>32</sup>P. McQuillan and J. Gomati, *J. Phys. Chem.* **100**, 5157 (1996).
- <sup>33</sup>V. A. Davydov, V. S. Zykov, and T. Yamaguchi, *Macromol. Symp.* **160**, 99 (2000).
- <sup>34</sup>V. A. Davydov, N. Manz, O. Steinbock, V. S. Zykov, and S. C. Müller, *Phys. Rev. Lett.* **85**, 868 (2000).
- <sup>35</sup>V. A. Davydov, N. Manz, O. Steinbock, and S. C. Müller, *Europhys. Lett.* **59**, 344 (2002).
- <sup>36</sup>N. Manz, V. A. Davydov, S. C. Müller, and M. Bär, *Phys. Lett. A* **316**, 311 (2003).
- <sup>37</sup>N. Manz, *Untersuchung chemischer Wellen in der Belousov-Zhabotinski-Reaktion: räumlich modulierte Systeme und anomale Dispersion*, Dissertation—Otto-von-Guericke-Universität Magdeburg, 2002.
- <sup>38</sup>E. V. Shikin, *Handbook and Atlas of Curves* (Chemical Rubber Corp., Boca Raton, FL 1995).
- <sup>39</sup>K. Kurin-Csörgei, I. Szalai, and E. Korös, *React. Kinet. Catal. Lett.* **54**, 217 (1995).
- <sup>40</sup>A. M. Pertsov, R. R. Aliev, and V. I. Krinsky, *Nature (London)* **345**, 419 (1990).
- <sup>41</sup>U. Storb, C. R. Neto, M. Bär, and S. C. Müller, *Phys. Chem. Chem. Phys.* **5**, 2344 (2003).
- <sup>42</sup>O.-U. Kheowan, V. S. Zykov, O. Rangsiman, and S. C. Müller, *Phys. Rev. Lett.* **86**, 2170 (2001).
- <sup>43</sup>K. V. McCloud and J. V. Maher, *Phys. Rep.* **260**, 139 (1995).
- <sup>44</sup>A. DeWit and G. M. Homsy, *J. Chem. Phys.* **107**, 9609 (1997).
- <sup>45</sup>H. Itoh, J. Wakita, T. Matsuyama, and M. Matsushita, *J. Phys. Soc. Jpn.* **68**, 1436 (1999).